Mallikarjuna et al. Protection and Control of Modern Power Systems (2018) 3:12
https://doi.org/10.1186/s41601-018-0087-z

Protection and Control of Modern Power Systems

ORIGINAL RESEARCH Open Access

PMU based adaptive zone settings of distance relays for protection of multi-terminal transmission lines

Balimidi Mallikarjuna[1], Pudi Shanmukesh[1], Dwivedi Anmol[1], Maddikara Jaya Bharata Reddy[1*] and Dusmanta Kumar Mohanta[2]

Abstract

This paper proposes Phasor Measurement Unit (PMU) based adaptive zone settings of distance relays (PAZSD) methodology for protection of multi-terminal transmission lines (MTL). The PAZSD methodology employs current coefficients to adjust the zone settings of the relays during infeed situation. These coefficients are calculated in phasor data concentrator (PDC) at system protection center (SPC) using the current phasors obtained from PMUs. The functioning of the distance relays during infeed condition with and without the proposed methodology has been illustrated through a four-bus model implemented in PSCAD/EMTDC environment. Further, the performance of the proposed methodology has been validated in real-time, on a laboratory prototype of Extra High Voltage multi-terminal transmission lines (EHV MTL). The phasors are estimated in PMUs using NI cRIO-9063 chassis embedded with data acquisition sensors in conjunction with LabVIEW software. The simulation and hardware results prove the efficacy of the proposed methodology in enhancing the performance and reliability of conventional distance protection system in real-time EHV MTLs.

Keywords: Extra high voltage (EHV), Multiterminal transmission line (MTL), Phasor measurement unit (PMU), Phasor data concentrator (PDC), Current coefficients

1 Introduction

Transmission lines are occassionally tapped to provide intermediate connections to loads or reinforce the underlying lower voltage network through a transformer. Such a configuration is known as multi-terminal transmission lines. For strengthening the power system, MTLs are frequently designed as a temporary and inexpensive measure. However, they can cause problems in the protective system [1].

As a part of a continuous endeavor to eliminate the problems caused by MTLs and enhance the reliability of the protective system, many protection methodologies have been developed. A few of them are discussed here. Abe et al. [2] developed asynchronous measurements based protection methodology for fault location in MTLs. The MTLs have been transformed into two terminal lines to achieve fault location accurately. Nagasawa et al. [3] have proposed an algorithm for protection of parallel MTLs using asynchronous differential currents at each terminal. Though the algorithms proposed by the authors [2, 3] performed well, their accuracy may be affected by unbalance in the line parameters when different fault conditions occur. Funbashi et al. [4] have proposed methods to identify the fault point in double circuit MTL using measurements from capacitor voltage transformer (CCVT) and current transformer (CT). However, for accurate fault location, measurements are required from all the terminals. In [5], Qiu et al. have developed a multi-agent algorithm for protection of MTLs. It consists of organization agent, coordination agent and executive agent. They exchange the information among themselves regarding trip information. However, lack of global synchronous measurements acquired from different agents may lead to mal-operation of the relay. Gajic et al. [6] have proposed differential protection with innovative charging current compensation algorithm for MTL

* Correspondence: jayabharat_res@yahoo.co.in
[1]Department of Electrical and Electronics Engineering, National Institute of Technology, Tiruchirappalli 620015, Tamil Nadu, India
Full list of author information is available at the end of the article

protection. However, the reliability of the algorithm depends on the availability of the current channels.

Forford et al. [7] have designed differential current algorithm for protection of MTLs. The proposed algorithm can differentiate internal fault, external fault and normal load conditions using electric mid-point (EMP). Arbes [8] has developed differential line protection scheme for the protection of double lines, tapped lines and short lines. However, the performance of the proposed scheme [8] depends on the local voltage and current measurements. Al-Fakhri [9] has proposed differential protection methodology against internal and external faults using asynchronous measurements. Hussain et al. [10] have proposed a fault location scheme for MTLs using positive sequence voltage and current measurements. However, the synchronization process may be affected due to metering errors. For reliable operation of proposed methods [9, 10], the precise time synchronization of analog information between the line ends must be required for the differential calculation to be accurate.

In addition to voltage and current based methodologies [2–10], traveling wave-based protection schemes have been proposed for MTL protection [11, 12]. Authors of [11] have used single traveling wave and fundamental measurements for fault location in MTLs. However, the performance of the methodology will be affected by arcing faults and variation in fault impedance. In [12], Zhu et al. developed a current traveling wave based algorithm. Fault detection and location functions are accomplished using arrival time of current waves at a terminal.

Technological developments in measurements, communication, control and monitoring of power grids have brought a paradigm shift in the protection philosophy of transmission lines. The reliability of power system has been enhanced by early detection of wide-area disturbances and optimal utilization of assets. Some of the protection methodologies based on Synchrophasor measurements are discussed here. Lin et al. [13] demonstrated the performance of PMU based fault location algorithm on MTLs. Faults are identified and located using synchronized positive sequence voltage and current phasors. Further, for accurate fault detection and location in MTLs, Brahma [14] has employed time-stamped voltage and current phasors obtained from all the terminals. Ting Wu et al. [15] have formed a novel fault location technique for multi-section non-homogeneous transmission lines. However, the accuracy of [14, 15] may be lost in case of medium and long MTLs. For decades, the distance protection is widely employed for the protection of transmission lines as it is simple and fast. The distance protection can protect most of the protected line, and it is virtually independent of the source impedance. However, the performance and the reliability of the distance protection are influenced by infeed and outfeed currents in MTLs [16–18].

In this paper, PMU based adaptive zone settings of distance relays (PAZSD) methodology has been proposed to improve the performance and the reliability of distance protection by adjusting zone settings adaptively. The PAZSD methodology employs current coefficients to adjust the zone settings of the distance relays during infeed situations. These coefficients are calculated in phasor data concentrator (PDC) at system protection center (SPC) using the magnitude of current phasors obtained from PMUs. The functioning of the distance relays during infeed condition with and without the proposed methodology has been demonstrated through different fault case studies carried out on a four-bus model in PSCAD/EMTDC environment. Further, a laboratory prototype of EHV MTLs is considered to validate the performance of distance relays during infeed condition. For phasor estimation, PMUs are realized in real-time using NI cRIO-9063 chassis embedded with data acquisition sensors (NI-9225 & NI-9227) and Global Positioning System (GPS) synchronisation module (NI-9467) in conjunction with LabVIEW software. The results indicate that the proposed PAZSD methodology can improve the performance and the reliability of conventional distance protection during infeed situations under different fault conditions.

2 Synchrophasor Technology

The cutting-edge Synchrophasor technology entails estimation of time-stamped phasor measurements on GPS time reference. It has been used to provide accurate information regarding the state of the power system for implementing immediate corrective actions. The process of phasor estimation starts with a sampling of an analog signal (x(t)) at a sampling frequency f_s (= Nf_o). With this sampling frequency, N number of samples per cycle are obtained. The time-stamped fundamental phasors of three-phase voltage and current signals per cycle are estimated using the Discrete Fourier Transform (DFT) [19]. In general, the k^{th} estimation of the original signal is given by Eq. 1.

$$X_k = \frac{\sqrt{2}}{N}\sum_{n=0}^{N-1} x(n\Delta T)e^{-j\frac{2\pi kn}{N}} \quad (1)$$

where $x(n\Delta T)$ is sampled version of x(t) (voltage or current analog signals),

ΔT is sampling time in seconds,

f_o is nominal frequency (Hz),

T is time period in seconds,

N is number of samples per cycle,

n is sample number starting from $n = 0$ to N-1,

For $k = 1$, X_k gives the fundamental frequency phasor.

A concise description of the infeed problem encountered by distance protection in MTLs and proposed solution (PAZSD methodology) under different fault conditions are discussed in the following section.

3 Methods

Fig. 1 shows a part of an interconnected power system for illustrating the effect of infeed on the performance of distance relays. Let the distance relays protecting the lines *i-l* and *l-j* are R_{il} & R_{li}, and R_{lj} & R_{jl} respectively. Likewise, the distance relays of the teed terminal *l-k* are R_{lk} and R_{kl}. Assume PMUs are installed at all the buses which communicate to the PDC at SPC through a modem and fiber optical cables. Assuming the currents I_p and I_q are in phase. For illustration purpose, the PMUs at Bus *i* and *k* are considered.

3.1 Infeed effect

In order to explain the infeed effect, only relays are assumed to be present in the above power system network (No PMUs, PDC and SPC are present). Assume that a fault has occurred on the line *l-j* at a point D as shown in Fig. 1. The resultant currents are indicated in Fig. 1. Under such conditions, the impedance observed by the relay R_{il} at Bus *i* is obtained using KVL:

$$V_i = I_p(Z_{il} + Z_{lD}) + I_q Z_{lD} \tag{2}$$

$$\frac{V_i}{I_p} = (Z_{il} + Z_{lD}) + \frac{I_q}{I_p} Z_{lD} \tag{3}$$

Let $\quad Z_{il} + Z_{lD} = Z_{iD}$

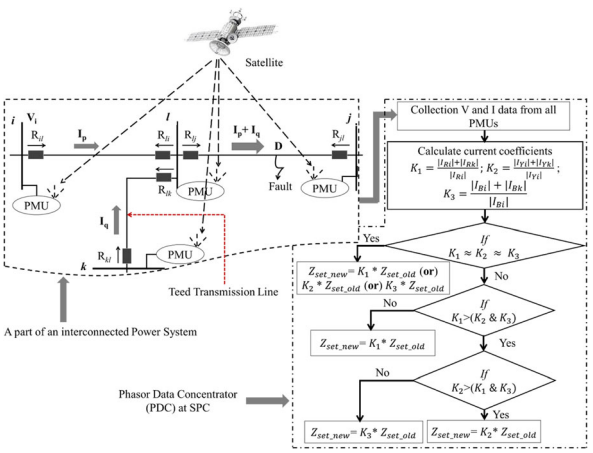

Fig. 1 Proposed PAZSD methodology for multi-terminal transmission lines (MTL)

$$\frac{V_i}{I_p} = Z_{iD} + \frac{I_q}{I_p} Z_{lD} \tag{4}$$

where.

V_i is voltage at a Bus *i*,

Z_{il} is the impedance of transmission line *i-l*,

Z_{lD} is impedance of transmission line *l-j* from Bus *l* to the fault point D,

I_p is current flowing from Bus *i* to *l*,

I_q is current flowing from Bus *k* to *l*,

From Eq. (4), it is observed that the impedance seen by the relay R_{il} is more than the impedance observed (Z_{iD}) when there is infeed. Therefore, the relay R_{il} under reaches during fault condition. The main cause for such phenomenon is that the relay R_{il} cannot sense the current (I_q) flowing from Bus *k* to *l*. The amount of under reach depends on the magnitude of current I_q.

To address the above infeed issue and to ensure reliable operation of the relay R_{il}, the subsequent section proposes the PAZSD methodology. This proposed methodology guides the relay to change the zone settings according to the infeed conditions using Synchrophasor technology. The PAZSD methodology which is executed in the PDC sends the new zone settings to the corresponding relay to ensure reliable operation during the infeed condition.

3.2 Flowchart of proposed PAZSD methodology

The sequence of execution of the proposed PAZSD methodology, as shown in Fig. 1, is illustrated in step by step manner to eliminate the infeed problem as discussed in the previous section.

Step 1: Synchronized time-stamped voltage and current phasor data are estimated in the PMU at Bus *i* and *k*, and transmitted to PDC at SPC.

Step 2: In PDC, three-phase current coefficients (K_1, K_2 and K_3) are calculated from the magnitudes of the current phasors using Eqs. (5) to (7)

$$K_1 = \frac{|I_{Ri}| + |I_{Rk}|}{|I_{Ri}|} \tag{5}$$

$$K_2 = \frac{|I_{Yi}| + |I_{Yk}|}{|I_{Yi}|} \tag{6}$$

$$K_3 = \frac{|I_{Bi}| + |I_{Bk}|}{|I_{Bi}|} \tag{7}$$

Step 3: If $K_1 \approx K_2 \approx K_3$, adjust the reach settings of the relay R_{il} using Eq. (8).

$$Z_{\text{set-new}} = K_1^{*} Z_{\text{set-old}} \tag{8}$$

Else if $K_1 > (K_2 \,\&\, K_3)$, adjust the reach settings of the relay R_{il} using Eq. (9).

$$Z_{\text{set-new}} = K_1{}^{*}\, Z_{\text{set-old}} \tag{9}$$

Else if K_2> (K_1 & K_3), adjust the reach settings of relay R_{il} as given in Eq. (10).

$$Z_{\text{set-new}} = K_2{}^{*}\, Z_{\text{set-old}} \tag{10}$$

Else adjust the reach settings of the relay R_{il} as given in Eq. (11).

$$Z_{\text{set-new}} = K_3{}^{*}\, Z_{\text{set-old}} \tag{11}$$

where.

K_1, K_2, K_3 are current cofficients for infeed condition,

I_{Ri}, I_{Yi} & I_{Bi} are three-phase current phasors flowing from Bus i to l,

I_{Rk}, I_{Yk} & I_{Bk} are three-phase current phasors flowing from Bus k to l,

$Z_{\text{set-old}}$ are old three zone reach settings of the relay R_{il},

$Z_{\text{set-new}}$ are new three-zone reach settings of the relay R_{il} with infeed line (between Bus k and l).

The following section describes the implementation of the proposed PAZSD methodology on a four-bus system to eliminate the infeed problems as discussed in section 3.1.

3.3 Case studies

A four-bus model shown in Fig. 2 is considered and implemented in PSCAD/EMTDC software. Various case studies (Case 1, Case 2 and Case 3) are conducted to illustrate the functioning of distance relays for infeed condition. The base MVA and kV of the system are 100 and 400 (line to line) respectively. The positive sequence resistance, inductive and capacitive reactance of the transmission line are 0.0234 Ω/km, 0.298 Ω/km, and 256. 7 kΩ*km respectively. The values of negative sequence parameters are same as that of the positive sequence parameters. Similarly, the values of zero sequence resistance, inductive and capacitive reactance of the transmission lines are 0.388 Ω/km, 1.02 Ω/km, and 376.6 kΩ*km respectively. The length of each transmission line is 350 km. The zone settings of the distance relays are given in Table 1. Assume PMUs are installed at all buses.

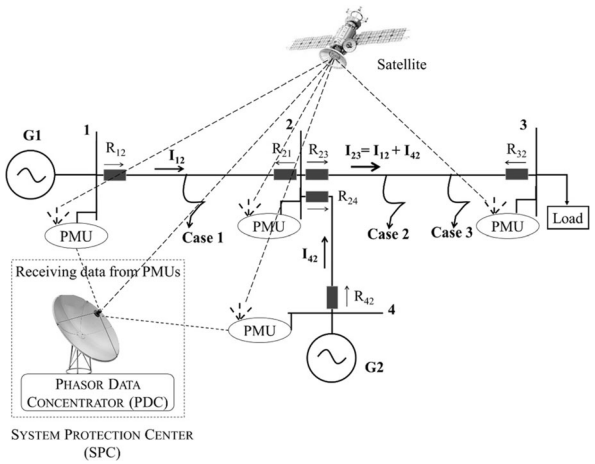

Fig. 2 A four-bus model implemented in PSCAD/EMTDC software to illustrate the functioning of the distance relays during infeed condition

3.3.1 Performance of distance relays without PAZSD methodology during infeed condition

Three case studies (Case 1, Case 2 and Case 3), as shown in Fig. 2, are considered to illustrate the performance of the distance relay R_{12} without PAZSD methodology. Assuming that no PMU, PDC and SPC technology are present in the case studies.

3.3.1.1 Case 1

Assume that a triple line fault (RYB) occurred at a distance of 10 km from Bus-1. In other words, in Zone-1 of the relay R_{12} and Zone-2 of the relay R_{21}. For such condition, the impedance trajectory of the distance relays, R_{12}, R_{21}, and R_{23}, is portrayed in Fig. 3.

From Fig. 3, the relays R_{12} and R_{21} have observed the impedance in Zone-1 and Zone-2 respectively. Whereas, the relay R_{23} has not observed the impedance in any of its zones. Hence, it is clear that none of the relays are affected by the infeed condition and the respective relays have correctly detected a fault condition.

3.3.1.2 Case 2

A double line to ground fault (RYG) is created at a distance of 500 km from Bus-1 (i.e., 150 km from Bus-2). This indicates the relays R_{12} and R_{23} should detect the fault in Zone-2 and Zone-1 respectively. The corresponding impedance trajectory of the relays R_{12}, R_{21} and R_{23} is shown in Fig. 4. From Fig. 4, it is observed that the relay R_{12} has observed the trajectory in Zone-3 whereas the relay R_{23} has observed in Zone-1. The relay R_{21} has not observed the trajectory in any of its zone due to its inherent directional property. Therefore, it is understood that the infeed at Bus-2 has caused the relay R_{12} to mal-operate.

3.3.1.3 Case 3

A double line fault (RY) is created at a distance of 200 km from Bus-2 which lies in Zone-3 of the relay R_{12} and Zone-1 of the relay R_{23}. For this event, impedance trajectory observed by the relays, R_{12}, R_{21} and R_{23} are shown in Fig. 5. From figure, it is concluded that the relays R_{12} and R_{21} have not seen the impedance in any of their zones. Whereas, the relay R_{23} has seen the impedance in Zone-1. Therefore, it is clearly known that the

Table 1 Zone settings of the distance relays

Relays	Zone-1	Zone-2	Zone-3
R_{12}, R_{21} & R_{23} R_{32}, R_{24} & R_{42}	6.552 + j83.44	12.285 + j156.45	17.199 + j219.03

infeed at Bus-2 has influenced the relay R_{12} to mal-operate.

From the above three case studies, it is clear that the performance of the relay is affected by the infeed at Bus-2 when a fault occurs on the line 2–3.

3.3.2 Performance of distance relays with proposed PAZSD methodology during infeed condition

The case studies discussed in the previous subsection are reconsidered with the implementation of the proposed PAZSD methodology using PMUs and PDC. The same four-bus system is considered, and the proposed PAZSD methodology is implemented in PDC at SPC with the data acquired from each PMU. Once the current coefficients (K_1, K_2, and K_3) are estimated in PDC, the new zone settings are calculated and communicated back to the corresponding relay. The following case studies prove the advantages of the proposed methodology to eliminate the infeed problem discussed in the previous section.

3.3.2.1 Case 1

A triple line fault (RYB) is created with the same fault conditions as discussed in section 3.3.1.1. The relay zone settings ($Z_{set\text{-}old}$) are shown in Table 2. The current coefficients (K_1, K_2, and K_3) and new zone settings estimated for the above fault condition are tabulated in Table 2 (according to the methodology proposed in section 3.2).

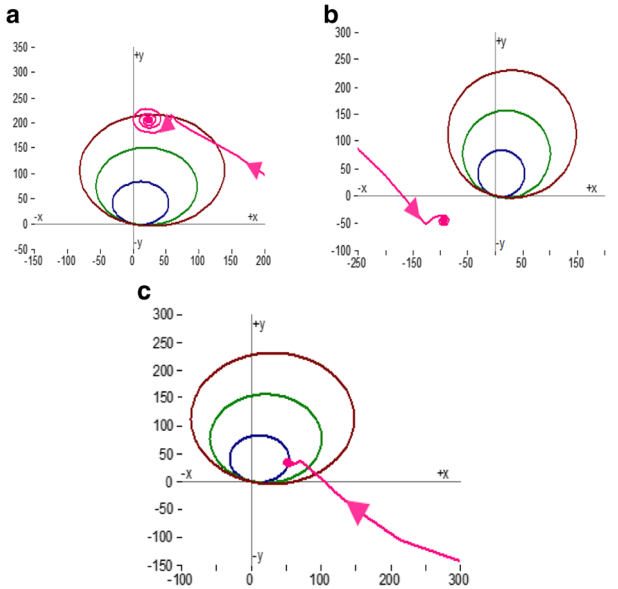

Fig. 4 Performance of (**a**) R_{12}, (**b**) R_{21} & (**c**) R_{23} for LLG (RYG) fault at 500 km from Bus-1 (i.e. 150 km from Bus-2)

These new zone settings are updated in the respective relays, and the relay operate as per the new settings. The impedance trajectory of the distance relays, R_{12}, R_{21}, and R_{23} is portrayed in Fig. 6. From Fig. 6, the relays R_{12} and R_{21} have observed the impedance in Zone-1 and Zone-2 respectively. Whereas, the relay R_{23} has not observed the impedance in any of its zones. Hence, it is clear that none of the relays are affected by the infeed condition and the respective relays have properly detected the fault condition with new zone settings.

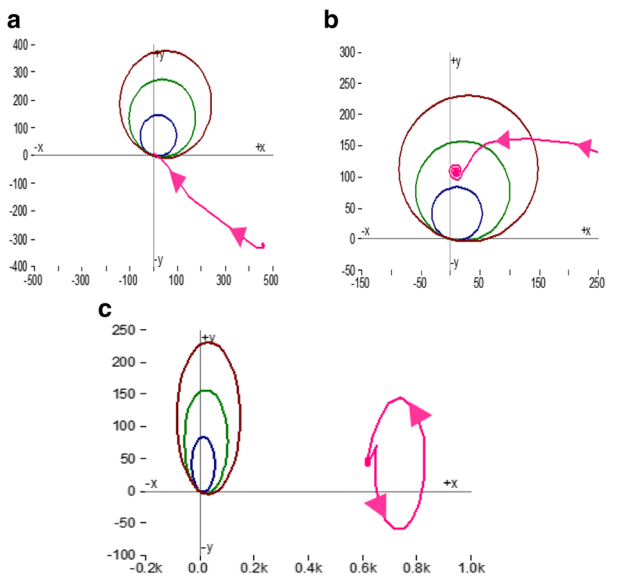

Fig. 3 Performance of (**a**) R_{12}, (**b**) R_{21} & (**c**) R_{23} for LLL (RYB) fault at 10 km from Bus-1 (Zone-1 of R_{12} and Zone-2 of R_{21})

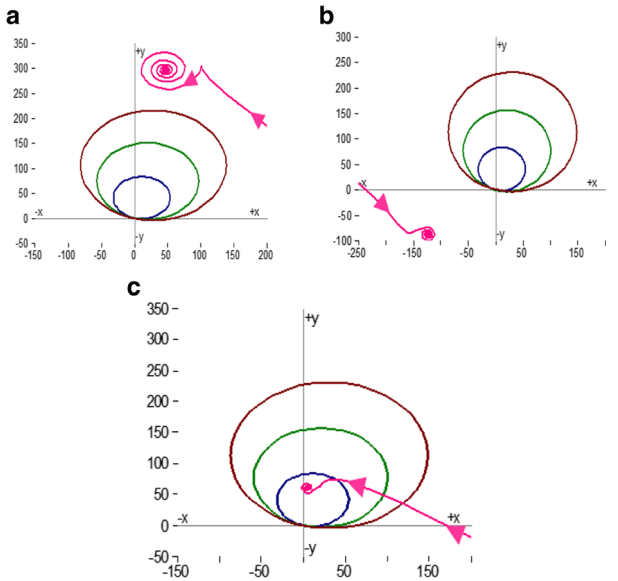

Fig. 5 Performance of (**a**) R_{12}, (**b**) R_{21} & (**c**) R_{23} for LL (RY) fault at 550 km from Bus-1 (i.e. 200 km from Bus-2)

Table 2 Zone settings of the distance relays, R_{12}, R_{21} & R_{23} using PAZSD methodology

Case studies	$Z_{set\text{-}old}$			Current Coefficient K_1, K_2 & K_3	$Z_{set\text{-}new}$ as per the proposed methodology		
	Zone-1	Zone-2	Zone-3		Zone-1	Zone-2	Zone-3
Case 1	6.552 + j83.44	12.285 + j156.45	17.199 + j219.03	49, 49 & 49	321.048 + j4088.56	601.965+ j7666.05	842.751+ j10732.47
Case 2				1.82, 1.79 & 1.9	12.449 + j158.536	23.342+ j297.255	32.678+ j416.157
Case 3				1.8, 1.78 & 1.89	12.383 + j157.702	23.219+ j295.691	32.506+ j413.967

3.3.2.2 Case 2

A double line to ground fault (RYG) is considered with same fault conditions as discussed in section 3.3.1.2. The estimated current coefficients (K_1, K_2, and K_3) and new zone settings and tabulated in Table 2. The values of current coefficients K_1, K_2 and K_3 are 1.82, 1.79 and 1.9 respectively. Since $K_3 > (K_1 \& K_2)$, as per the proposed methodology the new zone settings of the relay R_{12} ($Relay_{set\text{-}new} = K_3{*}Relay_{set\text{-}old}$) are 12.449 + j158.536, 23.342+ j297.255 and 32.678+ j416.157. The impedance trajectory of relays R_{12}, R_{21} and R_{23} are shown in Fig. 7, and it is clear that the relay R_{12} has detected the fault in Zone-2. From these case studies (3.3.1.2 & 3.3.2.2) it is observed that because of implementation of the proposed methodology, the relay R_{12} could detect the fault condition in Zone-2 (instead of Zone-3), which averts the mal-operation of the relay.

3.3.2.3 Case 3

A double line fault (RY) is considered with same fault conditions as discussed in section 3.3.1.3. The current coefficients (K_1, K_2, and K_3) and new zone settings estimated for the above fault condition are tabulated in Table 2. The values of the current coefficients K_1, K_2 and K_3 are 1.8, 1.78 and 1.89 respectively. Since $K_3 > (K_1 \& K_2)$, as per the proposed methodology the zone settings of the relay R_{12} ($Relay_{set\text{-}new} = K_3{*}Relay_{set\text{-}old}$) are 12.383 + j157.702, 23.219 + j295.691 and 32.506 + j413.967. The impedance trajectory is shown in Fig. 8 and it is clear that the relay R_{12} has detected the fault in Zone-3. From these case studies (3.3.1.3 & 3.3.2.3) it is observed that because of implementation of the proposed methodology the relay R_{12} could detect the fault condition properly in Zone-3, which averts the mal-operation of the relay.

From the above case studies, it is understood that the performance of the relay R_{12} is satisfactory with new zone settings when a fault occurs on the line 1–2. However, the performance of the relay R_{12} has been corrected by the proposed PAZSD methodology when a fault occurs on the line 2–3. Therefore, the performance of distance relay (R_{12}) has been enhanced during the infeed condition with the help of the proposed methodology.

In the subsequent section, the efficacy of the proposed PAZSD methodology in enhancing the performance and

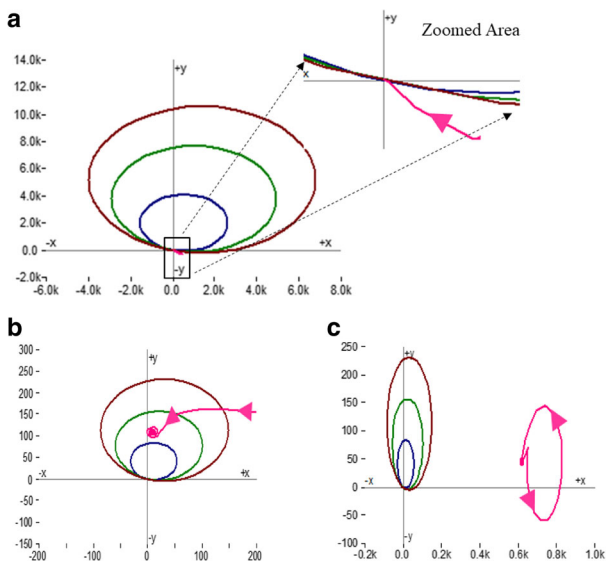

Fig. 6 Performance of (**a**) R_{12}, (**b**) R_{21} & (**c**) R_{23} for LLL (RYB) fault at 10 km from Bus-1 (Zone-1 of R_{12} and Zone-2 of R_{21}) with the proposed methodology

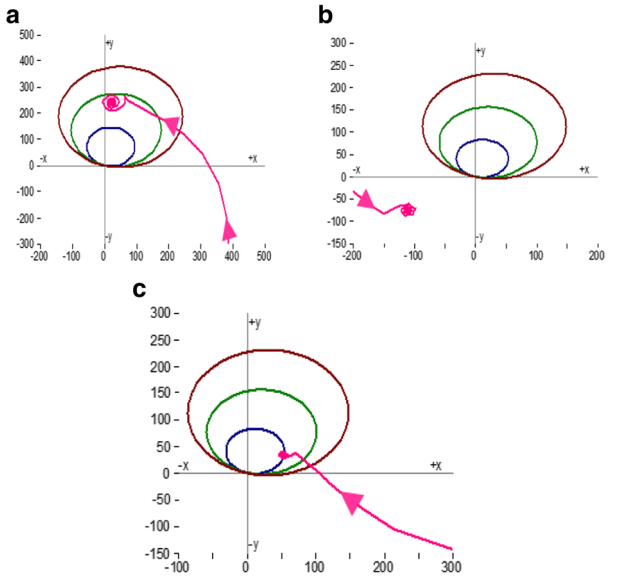

Fig. 7 Performance of (**a**) R_{12}, (**b**) R_{21} & (**c**) R_{23} for LLG (RYG) fault at 500 km from Bus-1 (i.e. 150 km from Bus-2) with the proposed methodology

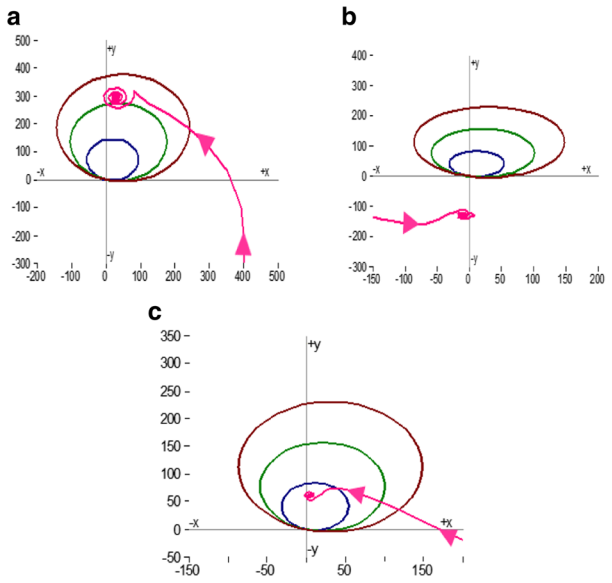

Fig. 8 Performance of (**a**) R_{12}, (**b**) R_{21} & (**c**) R_{23} for LL (RY) fault at 550 km from Bus-1 (i.e. 200 km from Bus-2) with the proposed methodology

reliability of the distance relay is validated in real-time on a laboratory prototype model of EHV MTL.

4 Results and discussion

A scale down laboratory prototype model of EHV MTL is shown in Fig. 9. As shown in figure, two three-phase 440 V, 50 Hz power supplies are connected to Bus B_1 and B_4 through autotransformers. The autotransformer steps down the supply voltage from 440 V to 110 V at 50 Hz. A three-phase variable load of 3.75 kW is connected at the receiving end (Bus B_3). PMUs are connected at all buses.

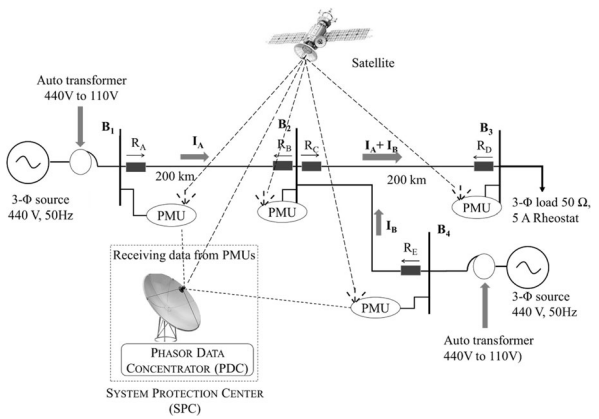

Fig. 9 Single line diagram of the scale down laboratory model of EHV MTL system for infeed condition

The length of the transmission lines 1–2 and 2–3 is 200 km each with the Π-model transmission line. Each 200 km transmission line is divided into four 50 km Π-sections connected in series. The parameters of the transmission line per 50 km are considered with resistance 1.8 Ω, inductance 10.07 mH and capacitance 2.2 μF. PMUs are implemented using NI cRIO-9063 chassis embedded with NI-9225 Voltage, NI-9227 Current and NI-9476 GPS modules programmed in LabVIEW FPGA software. As shown in Fig. 9, the three-phase voltage and current phasors are acquired from PMUs and communicated to the PDC. The sampling frequency of NI cRIO-9063 considered for phasor estimation is 2 kHz. To evaluate the performance of distance relay (R_A), numerous faults with different fault impedances (0.2 Ω, 1.7 Ω, and 4.9 Ω) are simulated and discussed in the following section.

4.1 Real-time performance analysis of the conventional distance relay without PAZSD methodology

The zone settings of the relay R_A are calculated for 400 km and tabulated in Table 3.

The following conditions are used to detect the zone of fault point.

$$\text{Zone-1}: \quad \text{If } |Z_{\text{Calculate-1}}| < 11.647 \tag{1}$$

where $|Z_{\text{Calculate-1}}|$ is the distance from the center of Zone-1 circle to the fault point.

$$\text{Zone-2}: \quad \text{If } 11.647 < |Z_{\text{Calculated-2}}| < 21.8388 \tag{2}$$

where $|Z_{\text{Calculate-2}}|$ is the distance from the center of Zone-2 circle to the fault point.

The performance of the distance relay R_A without the proposed methodology is evaluated for various faults with different fault impedances (0.2 Ω, 1.7 Ω and 4.9 Ω) and tabulated in Tables 4, 5 and 6.

From Table 4, for example, consider an LG fault occurred at 50 km from Bus B_1. The corresponding impedance observed by the relay R_A is $3.9612\angle 65.214^0$. The relay R_A has seen the impedance in Zone-1 since the magnitude of the impedance is less than 11.647 (Condition 1). Therefore, the relay operates as per its settings. Figure 10 displays the LabVIEW front panel for relay R_A in PDC at SPC (without the proposed methodology). For the case study, LabVIEW front panel displays a glowing LED for Zone-1 fault. Figure 10 also shows the voltage and current phasor data acquired from PMUs at B_1 and B_4, and the calculated impedance.

Table 3 Zone Settings of the distance relay R_A

Relays	Zone-1	Zone-2
R_A	$23.2947\angle 60.36^{\circ}\ \Omega$	$43.6776\angle 60.36^{\circ}\ \Omega$

Table 4 Performance of the distance relay R_A without PAZSD methodology for different faults with FR = 0.2 Ω at different distances

Fault Condition	Impedance seen by the relay R_A	Performance of R_A without proposed methodology	
		Zone of fault detection is?	Is detected zone correct? (Y/N)
LG Fault at 50 km	$3.9612 \angle 65.214^0$	Zone 1	Y
LL Fault at 50 km	$3.933 \angle 60.95^0$	Zone 1	Y
LLG Fault at 150 km	$11.765 \angle 58.05^0$	Zone 1	Y
LLL Fault at 150 km	$11.566 \angle 61.69^0$	Zone 1	Y
LG Fault at 250 km	$31.934 \angle 84.01^0$	Zone 2	N
LL Fault at 250 km	$32.092 \angle 84.44^0$	Zone 2	N
LLG Fault at 250 km	$35.082 \angle -273.07^0$	Zone 2	N
LLL Fault at 250 km	$34.394 \angle 84.89^0$	Zone 2	N
LLG Fault at 300 km	$48.136 \angle 80.37^0$	No Zone is detected	N
LG Fault at 350 km	$75.180 \angle 83.11^0$	No Zone is detected	N
LL Fault at 350 km	$82.706 \angle 83.21^0$	No Zone is detected	N
LLL Fault at 350 km	$76.616 \angle 79.09^0$	No Zone is detected	N

A similar explanation holds good for LL fault at 50 km, LLG & LLL faults at 150 km from Bus B_1 as given in Table 4.

Further, consider double line fault (LL) at 250 km from Bus B_1 as given in Table 4. The impedance observed by the relay R_A is $32.092\angle 84.44^0$. The relay R_A has seen the impedance in Zone-2 since the magnitude of the calculated impedance ($|Z_{Calculated\text{-}2}|$) is less than 21.8388 (Condition 2). Therefore, the relay operates in Zone-2 rather than in Zone-1. Thus, the infeed at Bus B_2 has caused the relay R_A to mal-operate. A similar explanation holds good for LG, LLG & LLL faults at 250 km from Bus B_1 as given in Table 4.

Furthermore, consider the double line to ground fault (LLG) at 300 km from Bus B_1 as given in Table 4. The impedance observed by the relay R_A is $48.136\angle 80.37^0$. The relay R_A has seen the impedance neither in Zone-1 nor in Zone-2 since the magnitude of the calculated impedance ($|Z_{Calculated}|$) is higher than 21.8388 (Condition 2). Therefore, the relay does not operate since the observed impedance has fallen out of its zone settings. Thus, the infeed at Bus B_2 has caused the relay R_A to mal-operate. A similar explanation holds good for LG, LL & LLL faults at 350 km from Bus B_1 as given in Table 4. The fault conditions for all the cases are shown in Table 4 considering a fault resistance of 0.2 Ω at the fault point.

Tables 5 and 6 show similar case studies as discussed in Table 4 but with different FR of 1.7 Ω and 4.9 Ω respectively. From tables, it is clear that with the change in FR the relay R_A malfunctions for many cases because of infeed condition at Bus B_2. Few cases are discussed below.

Consider double line fault (LL) at 250 km from Bus B_1 as given in Table 5. The impedance observed by the relay R_A is $32.092\angle 84.44^0$. The relay R_A has seen the impedance in Zone-2 since the magnitude of the calculated impedance ($|Z_{Calculated\text{-}2}|$) is less than 21.8388 (Condition 2). Therefore, the relay operates in Zone-2

Table 5 Performance of distance relay R_A without PAZSD methodology for different faults with FR = 1.7 Ω at different distances

Fault Condition	Impedance seen by the relay R_A	Performance of R_A without proposed methodology	
		Zone of fault detection is?	Is detected zone correct? (Y/N)
LL Fault at 50 km	$4.496 \angle 47.98^0$	Zone 1	Y
LLG Fault at 50 km	$3.895 \angle 59.41^0$	Zone 1	Y
LG Fault at 150 km	$14.445 \angle 53.48^0$	Zone 1	Y
LL Fault at 150 km	$11.114 \angle 54.07^0$	Zone 1	Y
LL Fault at 250 km	$32.092 \angle 84.44^0$	Zone 2	N
LLG Fault at 250 km	$32.444 \angle 51.75^0$	Zone 2	N
LLG Fault at 300 km	$53.717 \angle 87.03^0$	No Zone is detected	N
LLL Fault at 300 km	$50.457 \angle 79.35^0$	No Zone is detected	N
LLG Fault at 350 km	$81.044 \angle 61.89^0$	No Zone is detected	N
LLL Fault at 350 km	$76.823 \angle 76.77^0$	No Zone is detected	N

Table 6 Performance of distance relay R_A without PAZSD methodology for different faults with FR = 4.9 Ω at different distances

Fault Condition	Impedance seen by the relay R_A	Performance of R_A without proposed methodology	
		Zone of fault detection is?	Is detected zone correct? (Y/N)
LLG Fault at 50 km	$3.937 \angle 63.99^0$	Zone 1	Y
LLL Fault at 50 km	$8.436 \angle 22.5^0$	Zone 1	Y
LG Fault at 150 km	$20.52 \angle 45.07^0$	Zone 1	Y
LL Fault at 150 km	$16.296 \angle 43.51^0$	Zone 1	Y
LL Fault at 250 km	$38.814 \angle 68.43^0$	Zone 2	N
LLL Fault at 250 km	$39.5 \angle 67.69^0$	Zone 2	N
LLG Fault at 300 km	$52.864 \angle -273.09^0$	No Zone is detected	N
LLL Fault at 300 km	$52.268 \angle 65.303^0$	No Zone is detected	N
LG Fault at 350 km	$79.285 \angle 68.28^0$	No Zone is detected	N
LLG Fault at 350 km	$80.335 \angle 68.63^0$	No Zone is detected	N

rather than in Zone-1. Thus, the infeed at Bus B_2 has caused the relay R_A to mal-operate. Figure 11 displays the LabVIEW front panel for relay R_A in PDC at SPC (without the proposed methodology). The LabVIEW front panel displays glowing LED for Zone-2 fault. Figure 11 also shows the voltage and current phasor data acquired from PMUs at B_1 and B_4 and the calculated impedance.

Consider a double line to ground fault (LLG) with FR of 4.9 Ω at 350 km from Bus B_1 as given in Table 6. The impedance observed by the relay R_A is $80.335 \angle 68.63^0$.

The relay R_A malfunctions because the impedance observed by the relay is greater than 21.8388 (distance from the center of the Zone-2 circle to the fault point). A LabVIEW front panel display for this case study is shown in Fig. 12. Figure 12 also displays the LabVIEW front panel for relay R_A in PDC (without the proposed methodology). The voltage and current phasor data acquired from PMUs at B_1 and B_4, and the calculated impedances are also shown in Fig. 12.

The subsequent section presents the performance of the distance relay R_A when the proposed methodology has been implemented at SPC.

4.2 Real-time performance analysis of the conventional distance relay with PAZSD methodology

The following conditions are used to detect the zone of fault point using the proposed PAZSD methodology.

$$\text{Zone-1}: \quad \text{If } |Z_{\text{Calculate-1}}| < (|Z_{\text{new-Zone1}}|/2) \tag{3}$$

$$\text{Zone-2}: \quad \text{If } (|Z_{\text{new-Zone1}}|/2) < |Z_{\text{Calculated-2}}| < (|Z_{\text{new-Zone2}}/2) \tag{4}$$

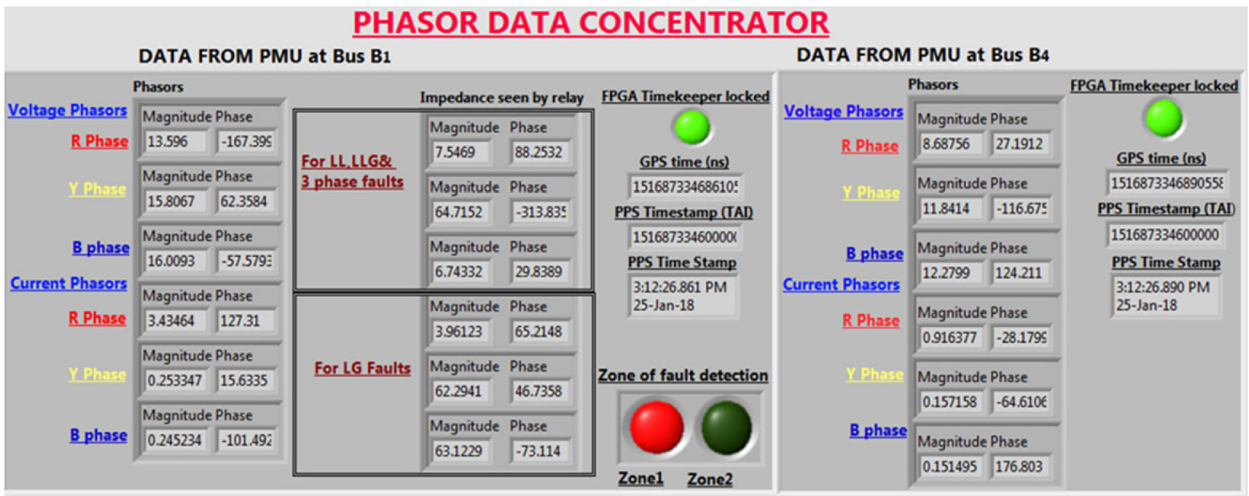

Fig. 10 LabVIEW front panel display of PDC at SPC showing the performance of distance relay R_A without the proposed PAZSD methodology for LG fault (FR = 0.2 Ω) at 50 km from B_1

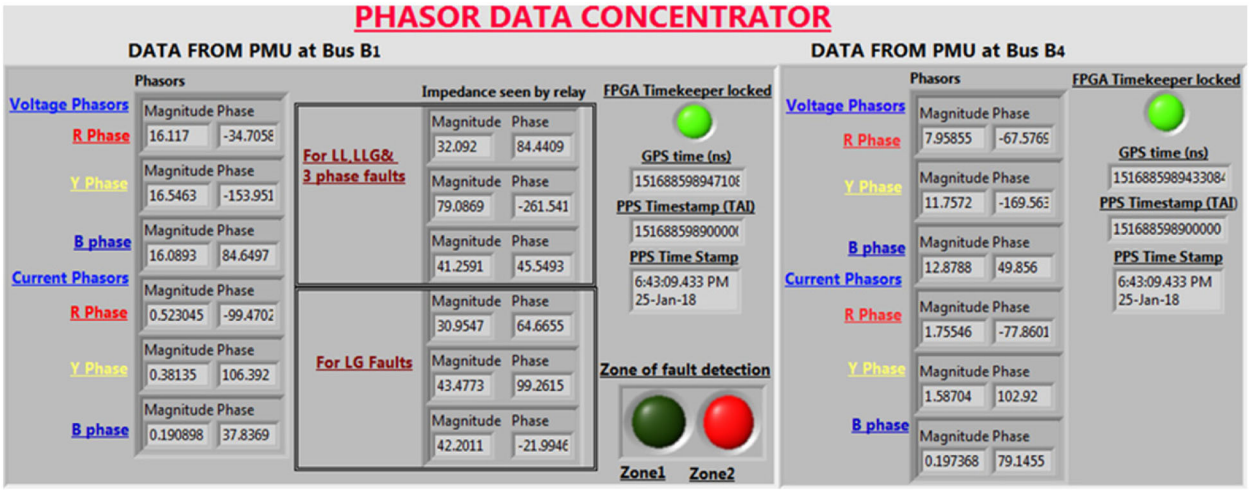

Fig. 11 LabVIEW front panel display of PDC at SPC showing the performance of distance relay R_A without the proposed PAZSD methodology when an LL fault (FR = 1.7 Ω) occurs at 250 km from B_1

In this subsection, the enhanced functioning of the distance relay R_A with PAZSD methodology for the same case studies (studied in subsection 4.1) is discussed. The new zone settings of the relay R_A using the current coefficients (K_1, K_2 & K_3) for different faults with different fault conditions are tabulated in Tables 7, 8 and 9.

From Table 7, for the LG with the same fault conditions as discussed in subsection 4.1, the current coefficients K_1, K_2 & K_3 estimated by the proposed methodology are 1.2656, 1.6712 & 1.5703 respectively. Since $K_2 > (K_1$ & $K_3)$, the new zone settings of the relay R_A as per the proposed methodology are $38.930\angle 60.36^{\circ}$ and $72.994\angle 60.36^{\circ}$. For this condition, the impedance observed by the relay R_A is $4.011\angle 63.599^{0}$. The zone of fault detection is Zone-1 since the magnitude of the observed value is less than 18.29 (Condition 3). Therefore, the operation of the relay R_A with new zone settings is same as with the old zone settings. Figure 13 displays the LabVIEW front panel for relay R_A in PDC at SPC (with the proposed methodology). The LabVIEW front panel displays glowing LED against Zone-1 fault. Figure 13 also shows the voltage and current phasors acquired from PMUs at B_1 and B_4 and the calculated impedance. A similar explanation holds good for LL fault at 50 km, and LLG & LLL faults at 150 km from bus B_1 as given in Table 7.

Similarly, for double line fault (LL) with the same fault conditions as discussed in subsection 4.1, the current coefficients K_1, K_2 & K_3 estimated by the proposed methodology are 4.3359, 5.1328 and 2.0313 respectively. The new zone settings of the relay R_A as per the proposed

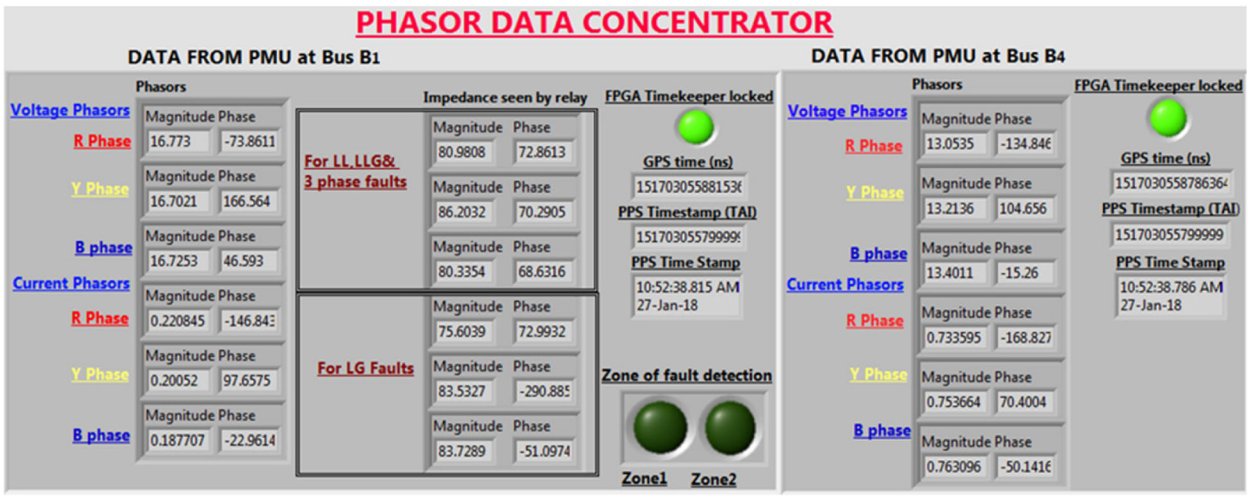

Fig. 12 LabVIEW front panel display of PDC at SPC showing the performance of distance relay R_A without the proposed PAZSD methodology for an LLG fault (FR = 4.9 Ω) at 350 km from B_1

Table 7 Performance of the distance relay R_A with PAZSD methodology for different faults with FR = 0.2 Ω at different distances

Fault Condition	Impedance seen by the relay R_A	Current Coefficients			New Zone Setting of		Performance of R_A with proposed methodology	
		K_1	K_2	K_3	Zone 1	Zone 2	Zone of fault detection is?	Is detected zone correct? (Y/N)
LG Fault at 50 km	$4.011\angle 63.599^0$	1.2656	1.6712	1.5703	$38.930\angle 60.36^\circ$	$72.994\angle 60.36^\circ$	Zone 1	Y
LL Fault at 50 km	$3.933\angle 60.95^0$	1.5703	1.3281	1.2734	$36.580\angle 60.36^\circ$	$68.587\angle 60.36^\circ$	Zone 1	Y
LLG Fault at 150 km	$11.765\angle 58.05^0$	2.8125	2.75	2.2422	$65.516\angle 60.36^\circ$	$65.516\angle 60.36^\circ$	Zone 1	Y
LLL Fault at 150 km	$11.566\angle 61.69^0$	1.7854	1.2134	1.6457	$41.59\angle 60.36^\circ$	$77.9827\angle 60.36^\circ$	Zone 1	Y
LG Fault at 250 km	$31.934\angle 84.01^0$	1.9766	4.8047	1.875	$111.924\angle 60.36^\circ$	$209.858\angle 60.36^\circ$	Zone 1	Y
LL Fault at 250 km	$32.092\angle 84.44^0$	4.3359	5.1328	2.0313	$119.567\angle 60.36^\circ$	$224.188\angle 60.36^\circ$	Zone 1	Y
LLG Fault at 250 km	$35.082\angle -273.07^0$	1.6484	2.2266	5.4453	$126.847\angle 60.36^\circ$	$237.838\angle 60.36^\circ$	Zone 1	Y
LLL Fault at 250 km	$34.394\angle 84.89^0$	4.9063	5.1719	5.7969	$135.037\angle 60.36^\circ$	$253.195\angle 60.36^\circ$	Zone 1	Y
LLG Fault at 300 km	$48.136\angle 80.37^0$	2.4688	4.0469	4.375	$101.914\angle 60.36^\circ$	$191.090\angle 60.36^\circ$	Zone 1	Y
LG Fault at 350 km	$75.180\angle 83.11^0$	2.8906	5.2188	2.7188	$121.570\angle 60.36^\circ$	$227.945\angle 60.36^\circ$	Zone 2	Y
LL Fault at 350 km	$82.706\angle 83.21^0$	2.6641	5.125	6.0469	$140.861\angle 60.36^\circ$	$264.114\angle 60.36^\circ$	Zone 2	Y
LLL Fault at 350 km	$76.616\angle 79.09^0$	4.9609	5.5234	5.8047	$128.666\angle 60.36^\circ$	$241.249\angle 60.36^\circ$	Zone 2	Y

methodology are $119.567\angle 60.36^\circ$ and $224.188\angle 60.36^\circ$ as $K_2 > (K_1$ & $K_3)$. For this condition, the impedance observed by the relay R_A is $32.092\angle 84.44^0$. The relay R_A has seen the impedance in Zone-1 since the magnitude of the calculated impedance ($|Z_{Calculated\text{-}1}|$) is less than 59.7835 (Condition 3). Therefore, the relay operates correctly, i.e. in Zone-1 whereas without the proposed methodology the relay R_A operates in Zone-2. Thus, the effect of the infeed on the relay R_A performance has been eliminated by the proposed methodology. A similar explanation holds good for LG, LL, LLG & LLL faults at 250 km from bus B_1 as given in Table 4. Likewise, for double line to ground fault (LLG) with the same fault conditions as discussed in subsection 4.1, the current coefficients K_1, K_2 & K_3 estimated by the proposed methodology are 2.4688, 4.0469 and 4.375 respectively. Since $K_3 > (K_2$ & $K_1)$, the new zone settings of the relay R_A using 4.375 are $101.914\angle 60.36^\circ$ and $191.090\angle 60.36^\circ$. The impedance observed by the relay R_A is $48.136\angle 80.37^0$.

The relay R_A has seen the impedance in Zone-1 since the magnitude of the calculated impedance ($|Z_{Calculated\text{-}1}|$) is less than 50.957 (Condition 3). Therefore, the relay does operate correctly, i.e. in Zone-1 whereas without the proposed methodology the relay R_A does not operate. Thus, the infeed at Bus B_2 has not affected the performance of the relay R_A. A similar explanation holds good for LG, LL & LLL faults at 350 km from Bus B_1 as given in Table 7. The fault conditions for all the cases are shown in Table 7 considering a FR of 0.2 Ω at the fault point.

Tables 8 and 9 show similar case studies as considered in Table 7 but with FR of 1.7 Ω and 4.9 Ω respectively. From tables, it is clear that with a change in FR the relay R_A with the proposed methodology functions correctly for

Table 8 Performance of distance relay R_A with PAZSD methodology for different faults with FR = 1.7 Ω at different distances

Fault Condition	Impedance seen by the relay R_A	Current Coefficients			New Zone Setting of		Performance of R_A with proposed methodology	
		K_1	K_2	K_3	Zone 1	Zone 2	Zone of fault detection is?	Is detected zone correct? (Y/N)
LL Fault at 50 km	$4.496\angle 47.98^0$	1.2813	1.2578	1.7422	$40.584\angle 60.36^\circ$	$76.095\angle 60.36^\circ$	Zone 1	Y
LLG Fault at 50 km	$3.895\angle 59.41^0$	1.5547	1.3125	1.2969	$36.216\angle 60.36^\circ$	$67.906\angle 60.36^\circ$	Zone 1	Y
LG Fault at 150 km	$14.445\angle 53.48^0$	2.6328	1.7969	2.2969	$61.330\angle 60.36^\circ$	$114.994\angle 60.36^\circ$	Zone 1	Y
LL Fault at 150 km	$11.114\angle 54.07^0$	2.7891	2.6406	2.0625	$64.971\angle 60.36^\circ$	$121.821\angle 60.36^\circ$	Zone 1	Y
LL Fault at 250 km	$31.75\angle -275.12^0$	4.3359	5.1324	2.0313	$119.558\angle 60.36^\circ$	$224.191\angle 60.36^\circ$	Zone 1	Y
LLG Fault at 250 km	$32.444\angle 51.75^0$	3.9063	2.0938	5.4219	$126.302\angle 60.36^\circ$	$236.816\angle 60.36^\circ$	Zone 1	Y
LLG Fault at 300 km	$53.717\angle 87.03^0$	2.2109	4.6016	5.1328	$119.567\angle 60.36^\circ$	$224.188\angle 60.36^\circ$	Zone 1	Y
LLL Fault at 300 km	$50.457\angle 79.35^0$	3.7734	2.2344	4.7109	$109.739\angle 60.36^\circ$	$205.761\angle 60.36^\circ$	Zone 1	Y
LLG Fault at 350 km	$81.044\angle 61.89^0$	2.7031	5.4375	5.3359	$126.665\angle 60.36^\circ$	$237.497\angle 60.36^\circ$	Zone 2	Y
LLL Fault at 350 km	$76.823\angle 76.77^0$	4.6797	5.1719	5.4922	$127.939\angle 60.36^\circ$	$239.886\angle 60.36^\circ$	Zone 2	Y

Table 9 Performance of distance relay R_A with PAZSD methodology for different faults with FR = 4.9 Ω at different distances

Fault Condition	Impedance seen by the relay R_A	Current Coefficients			New Zone Setting of		Performance of R_A with proposed methodology	
		K_1	K_2	K_3	Zone 1	Zone 2	Zone of fault detection is?	Is detected zone correct? (Y/N)
LLG Fault at 50 km	$3.937 \angle 63.99^0$	1.7266	1.3281	1.2969	$40.221\angle 60.36^\circ$	$75.414\angle 60.36^\circ$	Zone 1	Y
LLL Fault at 50 km	$8.436 \angle 22.5^0$	1.3281	1.3516	1.3906	$32.394\angle 60.36^\circ$	$60.738\angle 60.36^\circ$	Zone 1	Y
LG Fault at 150 km	$20.52 \angle 45.07^0$	2.5078	1.9219	2.1875	$58.418\angle 60.36^\circ$	$109.535\angle 60.36^\circ$	Zone 1	Y
LL Fault at 150 km	$16.296 \angle 43.51^0$	2.7656	2.5313	2.0703	$64.424\angle 60.36^\circ$	$120.795\angle 60.36^\circ$	Zone 1	Y
LL Fault at 250 km	$38.814 \angle 68.43^0$	1.7734	4.1172	4.7578	$110.832\angle 60.36^\circ$	$207.809\angle 60.36^\circ$	Zone 1	Y
LLL Fault at 250 km	$39.5 \angle 67.69^0$	3.3516	3.9453	4.3516	$101.369\angle 60.36^\circ$	$190.067\angle 60.36^\circ$	Zone 1	Y
LLG Fault at 300 km	$52.864 \angle -273.09^0$	2.2109	4.5156	5.1484	$119.930\angle 60.36^\circ$	$224.870\angle 60.36^\circ$	Zone 1	Y
LLL Fault at 300 km	$52.268 \angle 65.303^0$	3.5313	3.9063	4.6016	$107.193\angle 60.36^\circ$	$200.987\angle 60.36^\circ$	Zone 1	Y
LG Fault at 350 km	$79.285 \angle 68.28^0$	2.7891	4.5469	2.8516	$105.919\angle 60.36^\circ$	$198.598\angle 60.36^\circ$	Zone 2	Y
LLG Fault at 350 km	$80.614 \angle 68.66^0$	4.3359	4.75	5.0547	$117.748\angle 60.36^\circ$	$220.777\angle 60.36^\circ$	Zone 2	Y

all the cases regardless of the infeed condition at Bus B_2. Few cases are discussed below for better understanding.

From Table 8, consider double line fault (LL) with the same fault conditions as discussed in subsection 4.1 (Table 5). The current coefficients K_1, K_2 & K_3 estimated by the proposed methodology are 4.3359, 5.1328 and 2.0312 respectively. The new zone settings of the relay R_A as per the proposed methodology are $119.558\angle 60.36^\circ$ and $224.191\angle 60.36^\circ$ as $K_2 > (K_1$ & $K_3)$. The impedance observed by the relay R_A is $31.75\angle -275.12^0$. The relay R_A has seen the impedance in Zone-1 because the magnitude of the calculated impedance ($|Z_{\text{Calculated-1}}|$) is less than 59.77 (Condition 3). Therefore, the relay R_A with the proposed methodology does operate in the right zone, i.e. Zone-1 whereas without the proposed methodology the relay R_A operates in Zone-2. Thus, the mal-operation of the relay R_A is averted. Figure 14 displays the LabVIEW front panel for relay R_A in PDC at SPC (with the proposed methodology). The LabVIEW front panel displays glowing LED for Zone-1 fault. Figure 14 also shows the voltage and current phasor data acquired from PMUs at B_1 and B_4 and the calculated impedance. The fault conditions for all the cases are shown in Table 8 considering a FR of 1.7 Ω at the fault point.

Consider LLG fault with FR of 4.9 Ω at 350 km from Bus B_1 as given in Table 9. The current coefficients K_1, K_2 & K_3 estimated by the proposed methodology are 4.3359, 4.75 and 5.0547 respectively. The new zone

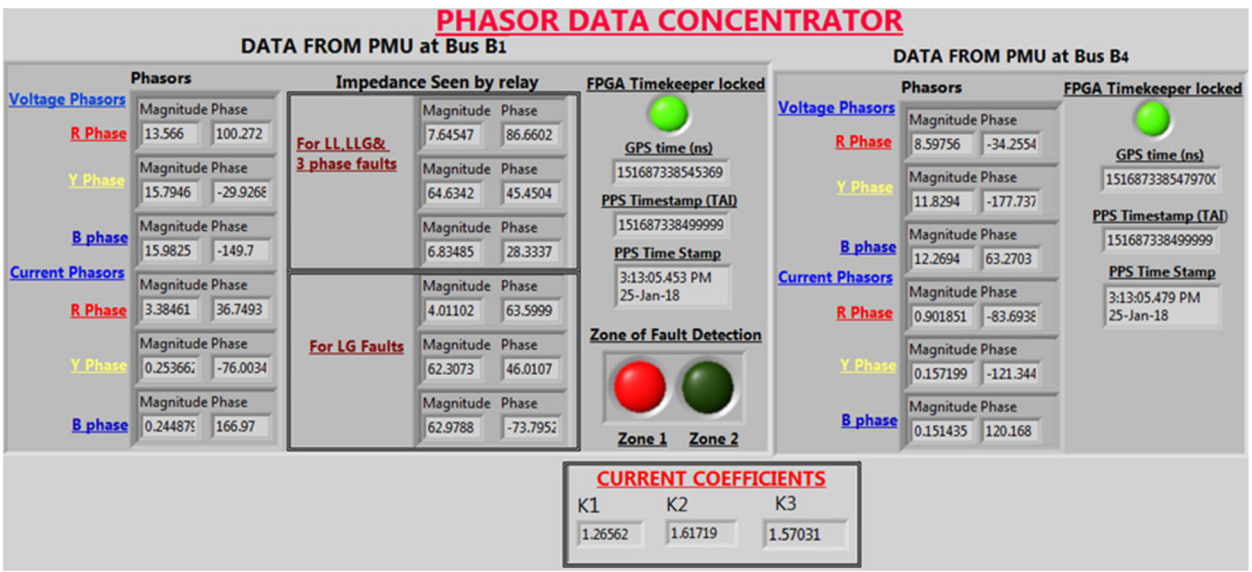

Fig. 13 LabVIEW front panel display of PDC at SPC showing the performance of distance relay R_A with the proposed PAZSD methodology for an LG fault (FR = 0.2 Ω) at 50 km from B_1

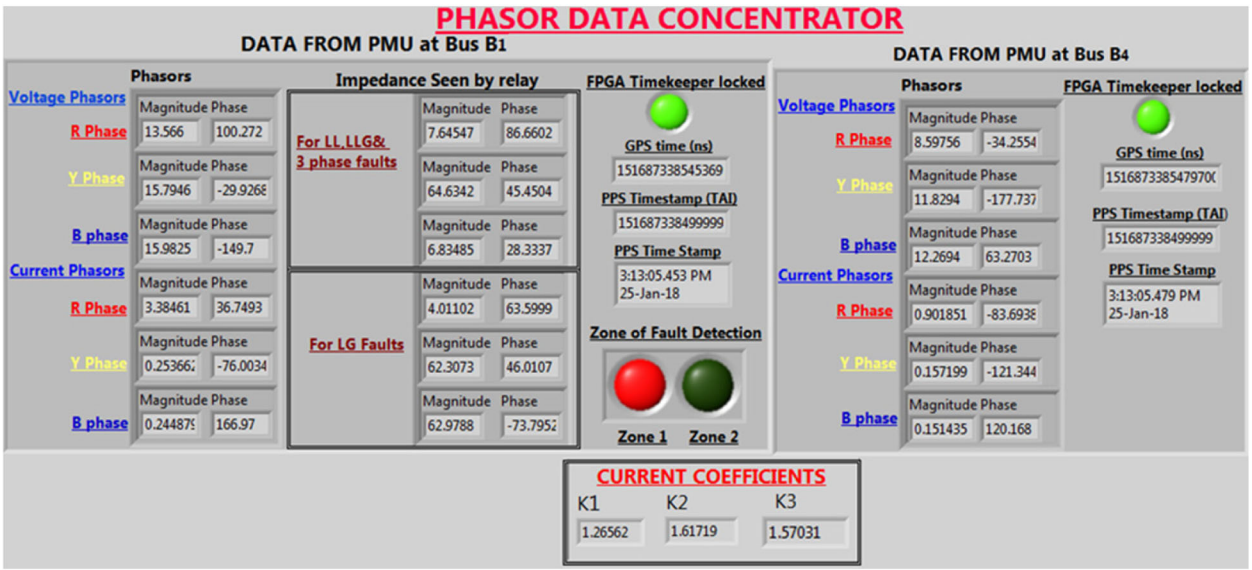

Fig. 14 LabVIEW front panel display of PDC at SPC showing the performance of distance relay R_A with the proposed PAZSD methodology for an LL fault (FR = 1.7 Ω) at 250 km from B_1

settings of the relay R_A as per the proposed methodology are $117.748\angle 60.36^{\circ}$ and $220.777\angle 60.36^{\circ}$ as $K_3 > (K_1$ & $K_2)$. The impedance observed by the relay R_A is $80.614\angle 68.66^{0}$. The relay R_A has seen the impedance in Zone-2 since the magnitude of the calculated impedance ($|Z_{\text{Calculated-2}}|$) is less than 110.389 (Condition 4). Therefore, the relay R_A with the proposed methodology does operate in the right zone, i.e., Zone-2 whereas without the proposed methodology the relay R_A does not operate. The LabVIEW front panel display for LLG fault with FR of 4.9 Ω at 350 km from Bus B_1 is shown in Fig. 15. Figure 15 also displays the LabVIEW front panel for relay R_A in PDC at SPC (with the proposed methodology). The voltage and current phasor data acquired from PMUs at B_1 and B_4, and the calculated impedances are also shown in Fig. 15. The fault conditions for all the cases are shown in Table 9 considering an FR of 4.9 Ω at the fault point.

Thus, from the above elaborated discussion, it is clear that the proposed PAZSD methodology has improved the performance of the conventional distance relay.

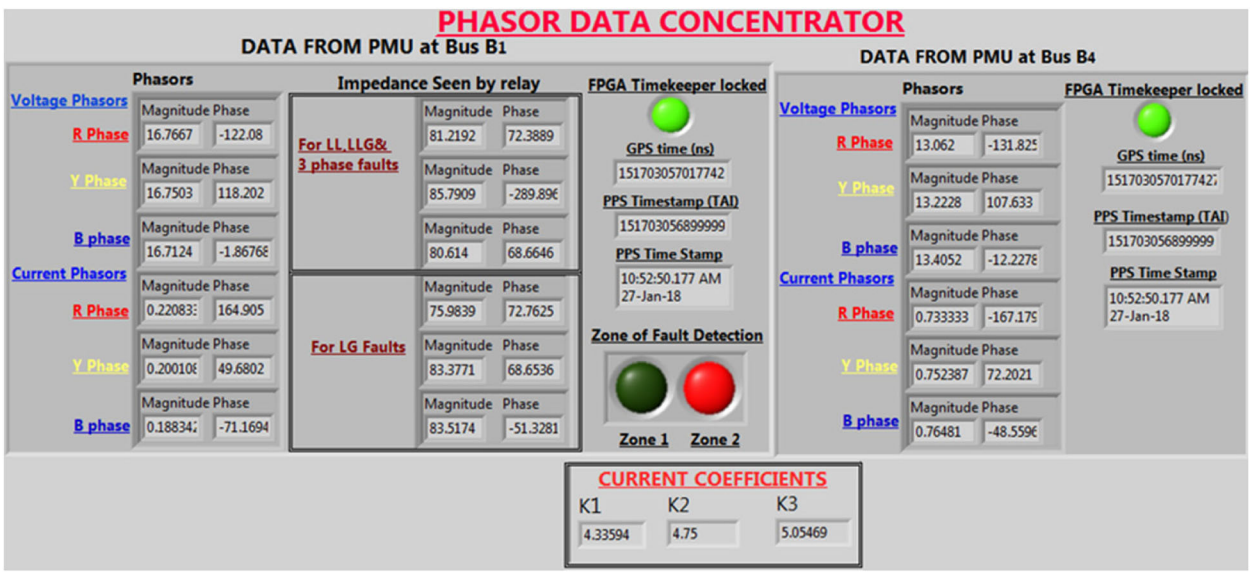

Fig. 15 LabVIEW front panel display of PDC at SPC showing the performance of distance relay R_A with the proposed PAZSD methodology for an LLG fault (FR = 4.9 Ω) at 350 km from B_1

4.3 Reliability analysis of the conventional distance protection without and with the proposed methodology

Despite the simple and dependable performance of the conventional distance protective system, the reliability of distance protection is affected when infeed condition exists in MTLs. In-feed conditions jeopardize security in the power system due to the non-adaptive property of distance protection system and provide an obscure view of the system conditions. Further, the function of the conventional distance protection may not be accurate for faults with different fault impedances.

The reliability attribute of the conventional distance protection with and without the proposed PAZSD methodology has been analyzed in this section as per the definition of reliability [19].

From Table 4, for instance, when an LL fault occurred at 50 km from Bus B_1, the relay R_A (without the proposed PAZSD methodology) has observed the fault point in Zone-1 which shows that the relay R_A operates correctly as per zone settings. Thus, the reliability attribute of the relay has not been influenced by the infeed at Bus B_2.

Similarly, the reliability of the relay had not influenced by the infeed when LG at 50 km, LLG & LLL faults at 150 km from Bus B_1 are separately created as given in Table 4. However, when LG fault occurred at 250 km from Bus B_1, the relay R_A has observed the fault in Zone-2, even though the fault is in Zone-1. Thus, the FR has influenced the reliability of the relay R_A. A similar explanation holds good for LG, LL, LLG & LLL faults at 250 km from Bus B_1 as given in Table 4. Likewise, when the double line to ground fault (LLG) occurred at 300 km from Bus B_1, the relay R_A has seen the impedance neither in Zone-1 nor Zone-2. Thus, the infeed at Bus B_2 and FR has influenced the reliability of the relay R_A. A similar explanation holds good for LG, LL & LLL faults at 350 km from Bus B_1 as given in Table 4.

Similarly, Tables 5 and 6 show similar case studies as discussed in Table 4 but with FR of 1.7 Ω and 4. 9 Ω respectively. From tables, it is clear that with the change in FR, the reliability of the relay R_A has been influenced by many cases because of infeed at Bus B_2. However, from Table 7, for the same fault conditions as discussed in Table 4, the reliability of the relay R_A has been improved by the proposed PAZSD methodology by changing the zone settings adaptively as per the requirement. Likewise, the reliability of the relay R_A has been improved by the proposed methodology for all the case studies as tabulated in Tables 8 to 9.

The above concise discussion underlines the importance of the proposed methodology in improving the reliability of conventional distance protection during infeed condition and impedance faults in MTLs.

5 Conclusions

This paper proposed a PMU based methodology for adaptive zone settings of distance relays to improve the performance and reliability of distance protection. The operation of distance relays during infeed condition with and without the proposed methodology has been demonstrated through a four-bus model implemented in PSCAD/EMTDC environment. Further, a laboratory prototype of EHV MTLs is considered to validate the performance of distance relays during infeed condition. The PAZSD methodology employs current coefficients to adjust the zone settings of the relays during infeed situations. The results strongly convey that the proposed PAZSD methodology is effective in improving the performance and reliability of distance protection during infeed condition.

Authors' contributions

BM has developed and implemented the proposed algorithm in hardware and simulation. Mr. Shanmukesh contributed towards hardware implementation and Mr. Anmol has contributed to develop the four bus power system model in PSCAD. MJBR has been the technical adviser for the total work and DKM has supported us in interpreting the simulation results and hardware results for eliminating the infeed effect in MTL. All authors have read and approved the final manuscript.

Competing interests

The authors declare that they have no competing interests.

Author details

[1]Department of Electrical and Electronics Engineering, National Institute of Technology, Tiruchirappalli 620015, Tamil Nadu, India. [2]Department of Electrical and Electronics Engineering, Birla Institute of Technology, Mesra, Ranchi 835215, India.

Received: 27 December 2017 Accepted: 26 April 2018
Published online: 12 May 2018

References

1. Al-Emadi, N. A., Ghorbani, A., & Mehrjerdi, H. (2016). Synchrophasor-based backup distance protection of multi-terminal transmission lines. *IET Generation, Transmission & Distribution, 10*(13), 3304–3313.
2. Abe, M., Otsuzuki, N., Emura, T., & Takeuchi, M. (1995). Development of a new fault location system for multi-terminal single transmission lines. *IEEE Transactions on Power Delivery, 10*(1), 159–168.
3. Nagasawa, T., Abe, M., Otsuzuki, N., Emura, T., Jikihara, Y., & Takeuchi, M. (1991). *Development of a new fault location algorithm for multi-terminal two parallel transmission lines* (pp. 348–362). Dallas, TX: Proceedings of the 1991 IEEE Power Engineering Society Transmission and Distribution Conference.
4. Funabashi, T., Otoguro, H., Mizuma, Y., Dube, L., & Ametani, A. (2000). Digital fault location for parallel double-circuit multi-terminal transmission lines. *IEEE Transactions on Power Delivery, 15*(2), 531–537.
5. Qiu, Z., Xu, Z., & Wang, G. (2006). *Relay protection for multi-terminal lines based on multi-agent technology* (pp. 7670–7673). Dalian: 6th World Congress on Intelligent Control and Automation.
6. Gajic, Z., Brncic, I., & Rios, F. (2010). *Multi-terminal line differential protection with innovative charging current compensation algorithm.* 10th IET international conference on developments in power system protection (DPSP 2010) (pp. 1–5). Manchester: Managing the Change.
7. Forford, T., Messing, L., & Stranne, G. (2004). *An analogue multi-terminal line differential protection.* 8th IEE International Conference on Developments in Power System Protection, *2*, 399–403.
8. Arbes, J. (1989). *Differential line protection application to multi-terminal lines* (pp. 121–124). Edinburgh: 1989 4th International Conference on Developments in Power Protection.
9. Al-Fakhri, B. (2004). *The theory and application of differential protection of multi-terminal lines without synchronization using vector difference as restraint*

quantity - simulation study. Eighth IEE International Conference on Developments in Power System Protection, *2*, 404–409.
10. Hussain, S., & Osman, A. H. (2016). Fault location scheme for multi-terminal transmission lines using unsynchronized measurements. *International Journal of Electrical Power & Energy Systems, 78*, 277–284.
11. Ngu, E. E., & Ramar, K. (2011). A combined impedance and traveling wave based fault location method for multi-terminal transmission lines. *International Journal of Electrical Power & Energy Systems, 33*(10), 1767–1775.
12. Zhu, Y., & Fan, X. (2013). Fault location scheme for a multi-terminal transmission line based on current traveling waves. *International Journal of Electrical Power & Energy Systems, 53*, 367–374.
13. Lien, K.-P., Liu, C.-W., Jiang, J. A., Chen, C.-S., & Yu, C.-S. (2005). *A novel fault location algorithm for multi-terminal lines using phasor measurement units* (pp. 576–581). Proceedings of the 37th Annual North American power symposium.
14. Brahma, S. M. (2005). Fault location scheme for a multi-terminal transmission line using synchronized voltage measurements. *IEEE Transactions on Power Delivery, 20*(2), 1325–1331.
15. Wu, T., Chung, C. Y., Kamwa, I., Li, J., & Qin, M. (2016). Synchrophasor measurement-based fault location technique for multi-terminal multi-section non-homogeneous transmission lines. *IET Generation, Transmission & Distribution, 10*(8), 1815–1824.
16. AIEE committee report. (1961). Protection of multiterminal and tapped lines. *Transactions of the American Institute of Electrical Engineers. Part III: Power Apparatus and Systems, 80*(3), 55–65.
17. Mir, M., & Hasan Imam, M. (1989). *Limits to zones of simultaneous tripping in multi-terminal lines* (pp. 326–330). Edinburgh: 4th International Conference on Developments in Power Protection.
18. Dinh, M. T. N., Bahadornejad, M., Shahri, A. S. A., & Nair, N. K. C. (2013). *Protection schemes and fault location methods for multi-terminal lines: A comprehensive review* (pp. 1–6). Bangalore: IEEE Innovative Smart Grid Technologies-Asia (ISGT Asia).
19. Phadke, A. G., & Thorpe, J. S. (2008). *Synchronized phasor measurements and their applications*. Springer: Power electronics and power systems series.